

# Initial ADAMS Analysis of the SOFIA Partial External Door System

James B. McConville  
Mechanical Dynamics, Inc.

Terry Arthur  
Raytheon Systems, Co.

## ABSTRACT

**NASA's Stratospheric Observatory for Infrared Astronomy (SOFIA) will employ a Boeing 747SP custom-modified to mount a 2.5 meter, infrared, reflecting telescope in the aft fuselage. The telescope requires a substantial cutout in the aft fuselage for the viewing aperture and a complex system of moving doors to seal the aperture when the telescope is not in use and to minimize the exposure of the telescope cavity to atmospheric effects when the telescope is in use. ADAMS has been employed to model the initial configuration of this Partial External Door System (PEDS) inclusive of component flexibility. As a result of the analysis, modifications to the system were proposed.**

## Background

Mechanical Dynamics, Inc. (MDI), Ann Arbor MI, were contracted by the Raytheon Systems Company (RSC), Waco TX, to develop and evaluate a flexible, articulating model of the proposed SOFIA Partial External Door System (PEDS) using the ADAMS Mechanical System Simulation (MSS) software[1]. RSC is tasked with constructing the proposed system and verifying its structural and functional integrity. The PEDS system is comprised of three, primary sub-systems:

- 1) The Upper Rigid Door (URD)  
A roller-mounted, external cover to the airframe cavity.
- 2) The Aperture Door (AD)  
A roller-mounted, contoured structure which provides a positionable viewing aperture for the telescope
- 3) The Flexible Door (FD)  
A roller-mounted, hinged, 9-segment assembly which seals the lower part of the cavity when the URD is open and the AD is elevated.

## Modeling Approach

A three-phased approach was employed in the modeling of the SOFIA PEDS:

### Phase 1 (Rigid - Rigid)

All structural door components were considered rigid as was the airframe mounting the system. Effort was concentrated on geometry collection from Pro-E and NASTRAN models and its transfer to ADAMS. The kinematic and kinetic characteristics of the door system were developed and a functioning ADAMS model was created and exercised in the time domain. Roller and gear drive forces for the system were determined as the components move through their kinematic envelopes in a benign, 1-G loading environment. Any, custom FORTRAN subroutines were generated (in initial form) and verified.

### Phase 2 (Flex – Rigid)

The articulating system components were rendered flexible using ADAMS FLEX\_BODIES derived from MSC/NASTRAN [3] structural models. The mounting airframe remained rigid. This system model was created from the Phase 1 model using ADAMS/VIEW [2] command files. The initial effects of structural compliance were introduced into the model and initial load estimates were available from this analysis.

### Phase 3 (Flex – Flex)

The airframe structure to be rendered flexible. This represents a substantial topological change from the previous 2 phases and requires extensive modification to the logic in the FORTRAN subroutines used to compute the roller contact forces. Because of system configuration changes subsequently proposed by NASA, this stage of the analysis was postponed.

## **URD Model**

In a structural sense, the URD is independent of the AD/FD assembly. It runs on a separate set of roller tracks, and has its own gear drive. The only physical contact between it and the other moving components consists of a 'catch' on the bottom edge of the door. In case of a drive system failure on the AD/FD assembly, it can engage a fitting on the upper edge of the AD and prevent an unwanted opening into the cavity from developing. For the analysis phases completed to date, this contact was not considered important and has not been modeled, permitting the URD analysis to be separated from the other components.

The ADAMS model was developed were using NASTRAN geometry, and a shell image of the supporting airframe was added to provide a reference for the articulating components (ref. fig. 1).

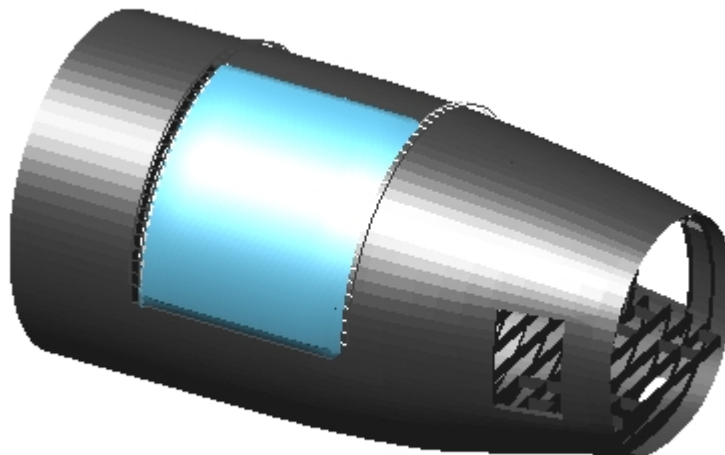


Fig 1. Phase 1 URD Model

## Model Topology - URD

The UDR(only) model consisted of four (4) components;

ground  
rear airframe  
URD  
URD drive pinion gear.

The aircraft coordinate system was used for all geometry input. Ground was the inertial reference frame for the model, while the remaining components were all modeled as (rigid) ADAMS PARTs. These components were interconnected using a combination of constraints (JOINTs), restraints (FORCEs), and applied loads (FORCEs) as follows:

airframe/ground –	FIX JOINT
pinion gear/airframe –	REVOLUTE JOINT
pinion gear/airframe --	MOTION
URD/airframe --	VFORCE (rollers -- qty. 46)
URD/pinion gear --	GFORCE (gear drive -- qty. 22)
URD/ground --	VFORCE (aero loads – qty 0)
URD.pinion.airframe/ground	(gravity)

### Constraints

The FIX joint secured the airframe to ground and is superfluous to the Rigid/Rigid analysis, since the door tracks could have equally well been modeled as a part of ground. The airframe was separated out at this stage only to make the later transition to flexibility easier. The REVOLUTE joint (ref. fig. 2) secures the door drive pinion gear to the airframe. The MOTION statement applies a velocity constraint to the remaining degree of freedom about the gear shaft axis.

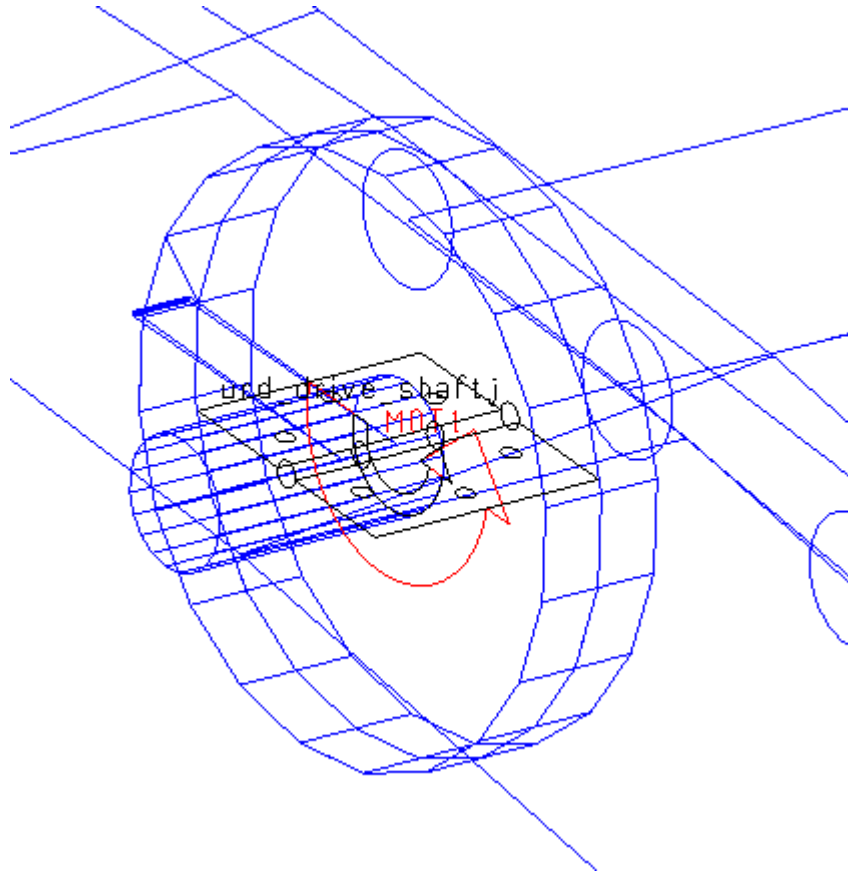


Fig. 2 URD Drive Pinion Gear and Motion Actuator

The sense of the revolute constraint (Joint/2) and the imposed motion (MOTION/1) are represented by the 'door hinge' and 'curl vector' graphics, respectively. The velocity is imposed by a standard ADAMS STEP function given as;

```
MOTION/1, ROTATIONAL, VELOCITY, JOINT = 2, FUNCTION = STEP(TIME,0,0,0.25,1.047)
```

This function represents an open-loop motion control which ramped the rotational velocity of the URD drive pinion gear from 0.0 rad/sec to 1.047 rad/sec over a time span of 0.25 simulation seconds using a Heavyside, faired cubic polynomial.

### Restraints

#### a)Rollers

The URD roller/airframe loads are modeled using ADAMS VFORCEs. A VFORCE applies (up to) three, mutually-orthogonal force components between two different bodies. In the ADAMS dataset, a typical radial roller force (ref. fig. 3) at the forward track is given by;

```
MARKER/ 21011,PART= 2, FLOAT
!          adams_view_name='VFO 21011'
VFORCE/ 21011,I=1011,JFLOAT= 21011,RM=1011,FUNCTION=USER(1,1011,1011, 21011,
, 2, 1, 1, 5000.0, 50.0)
!          adams_view_name='GRF 21011'
GRAPHICS/ 21011,FORCE,ETYPE=VFORCE,EID= 21011,EMARKER = 1011
```

Fig. 4 shows one of the two thrust rollers at the forward track position. It differs from the radial roller force only in terms of the FORCE, MARKER, and SPLINE IDs used to define it. The radial roller expression for VFORCE/21011 will be used as the basis of explanation for the roller forces in general.

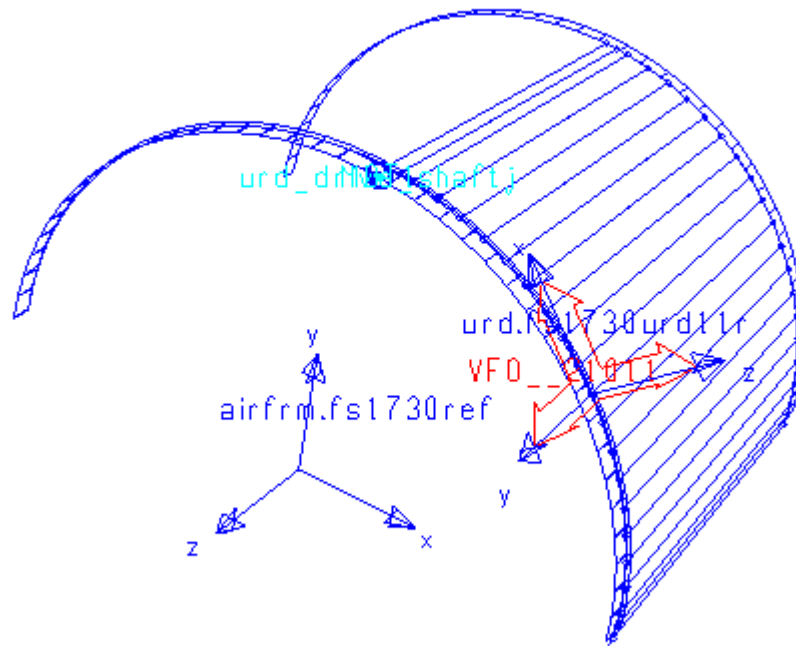


Fig. 3 Typical Radial Roller VFORCE at Forward URD Track

In ADAMS, a VFORCE is specified by an I-MARKER - a coordinate triad located on the I-PART to which the specified force is applied, an RM (reference) MARKER - specifying the directionality of the VFORCE, and a JFLOAT MARKER - a phantom point belonging to the J-PART upon which the reaction is to be applied but co-located and moving with the I-MARKER. The "FUNCTION = USER" entry on the VFORCE expression contains a string of parameters and denotes that the VFORCE algorithm is to be defined in a user-written subroutine rather than directly defined using ADAMS Data Language (ADL). Subroutines can employ C, C++, or FORTRAN77. In the present case, FORTRAN77 has been used.

PAR(1) = 1	a logical branch marker; 1 denotes radial roller forces
PAR(2) = 1011	a 4-digit force identifier
PAR(3) = 1011	I-MARKER identification
PAR(4) = 21011	JFLOAT MARKER identification
PAR(5) = 2	JPART identification
PAR(6) = 1	the ID of the spline containing the R, THETA coordinates of the radial track
PAR(7) = 1	the numerical ID of the spline center reference marker
PAR(8) = 5000	the (assumed) roller contact stiffness (lbf/in)
PAR(9) = 50	the (assumed) roller contact damping (lbf-sec/in)

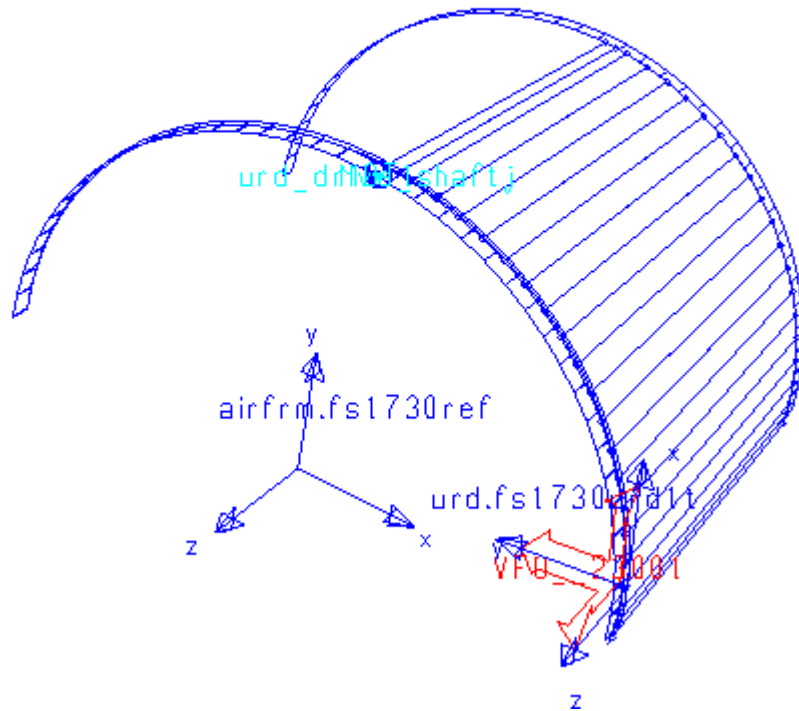


Fig. 4 Typical Thrust Roller VFORCE at Forward URD Track

The corresponding ADAMS dataset entries for the forward, radial roller spline and the spline reference marker (ref. fig. 3) are given below.

```
!                                adams_view_name='SPL1'
!                                adams_view_units='no_units'
SPLINE/1, X = 0, 30, 60, 90, 120, 150, 180, Y = 130.15, 130.15, 130.15, 130.15
, 130.15, 130.15, 130.15
!
!                                adams_view_name='fs1730ref'
MARKER/1, PART = 2, QP = 1753.29, 0, 231, REULER = 270D, 90D, 0D
```

In the spline, the (constant) radius of the track is input as Y-values vs. angular position (X-values) with respect to the spline reference marker (MARKER/1). In the analysis, the instantaneous position of the roller center (MARKER/1011) is accessed in global (XYZ-Cartesian) coordinates, converted to cylindrical coordinates. For the common theta-position, the R-position is compared against the spline. Using the RM MARKER (also MARKER/1011) for position and orientation, a Z-force (positive or negative, depending on MARKER/1011's position relative to the spline) is applied.

For the thrust rollers (Ref. fig. 4) the same scheme is used. For all the roller forces, a force graphics statement has been added as an aid to the visualization of the roller forces during the simulation.

## b) Pinion Gear Drive

Because the URD is not constrained to the airframe with constraints, the standard ADAMS GEAR statement cannot be employed. Instead, the pinion gear drive (ref. fig. 5) is modeled using a series of 6-

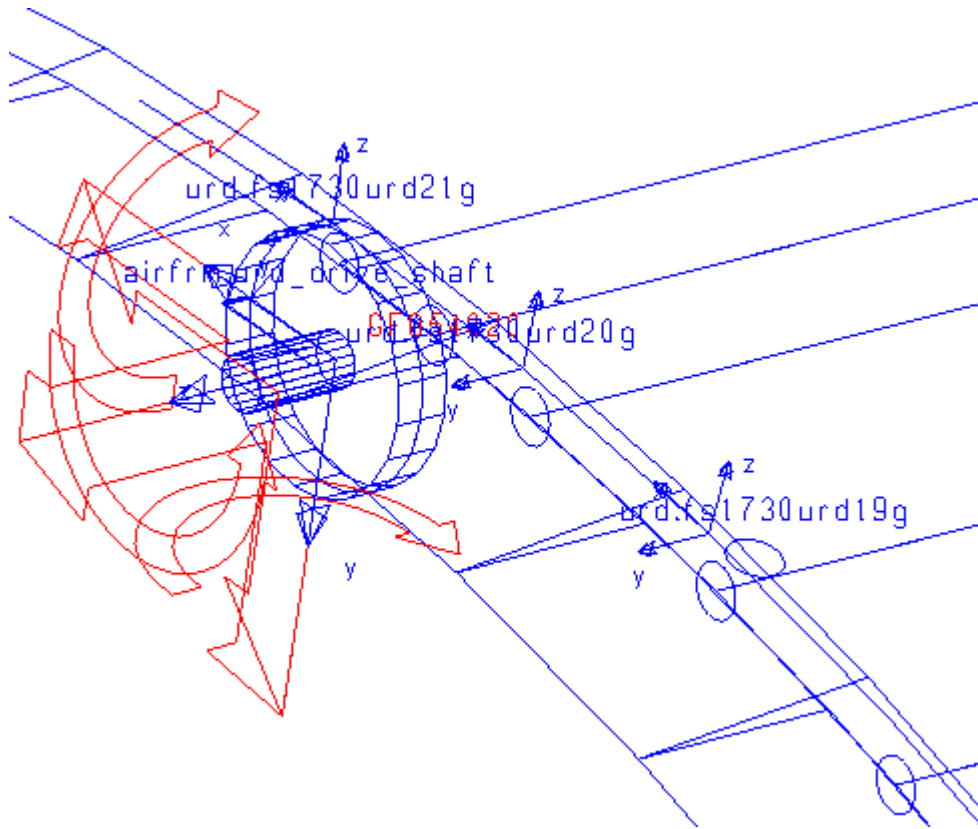


Fig. 5 Typical GFORCE Component of URD Gear Drive

component ADAMS GFORCEs which distribute the tangential gear drive force to the two sector gear points in closest proximity to the pinion gear center at any point in time. These forces have been implemented directly in the ADAMS dataset, and a sample is given below.

```
MARKER/54020,PART= 3, FLOAT
! adams_view_name='GFO54020'
GFORCE/54020,I=5,JFLOAT=54020,RM=4
,FX= -(0.25e5*(wz(5,4,4)*4.5-vx(4020,4,4)))
, *step(dx(4020,4,4),-10.129,0.0,0.0,1.0)
, *step(dx(4020,4,4),0.0,1.0,+10.129,0.0)\
,FY = 0\
,FZ = 0\
, TX = 0\
, TY = 0\
,TZ = -(-4.5*0.25e5*(wz(5,4,4)*4.5-vx(4020,4,4)))
, *step(dx(4020,4,4),-10.129,0.0,0.0,1.0)
, *step(dx(4020,4,4),0.0,1.0,+10.129,0.0)\
```

As is true in the case of the previously-described VFORCE, the ADAMS GFORCE employs a floating MARKER. In this instance, the floating marker is assigned to PART/3, which is the URD. The I-marker (ID = 5) is on the pinion, while the reference marker (ID = 4) is fixed to the airframe with its X-axis in the tangential direction and its Z-axis co-aligned with the spin axis of the pinion gear. In the "FX" component of the expression, "wz(5,4,4)\*4.5" generates the tangential velocity of the pinion gear rim by multiplying

the angular velocity of the pinion gear by its radius. This value is compared against the tangential velocity of the URD marker labeled "fs1730urd20g" (ID = 4020) and a large 'gain' force is applied to oppose any slip. In effect, the gear drive is modeled as a very low-slip friction wheel. The step functions ramp the tangential force from zero, when the contact is directly under fs1730urd21g", up to one when the contact is directly under "fs1730urd20g", and back down to zero when the contact point is directly under "fs1730urd19g". Thus, when the contact is between any two adjacent, gear reference points, the force is split between them, depending on the contact point's position in the gap. The torque force on the pinion gear ("TZ") is created by multiplying the tangential ("FX") force by the gear radius. There are 22 such GFORCES, all with the same I-marker, but each having a unique JFLOAT positioned along the arc of the sector gear on the URD.

### Applied Loading

#### a) Aerodynamic Force

(Aerodynamic loads not applied in Phase 1 analysis)

#### b) Gravity

The standard gravitational field of  $-386.088 \text{ in/sec}^2$  are applied to all PARTs.

## **Model Topology – AD/FD**

The AD-FD model is shown in fig. 7 (note: the airframe geometry has been omitted for clarity).

It consists of fifteen (15) components;

- ground
- rear airframe
- AD
- AD drive pinion gear.
- FD segments (qty 9)
- FD-AD links (qty 2)

The aircraft coordinate system is used for all geometry input. Ground is the inertial reference frame for the model, while the remaining components are all modeled as (rigid) ADAMS PARTs. These components are interconnected using a combination of constraints (JOINTs and joint primitives -- JPRIMs), restraints (FORCEs and BUSHINGs), and applied loads (FORCEs) as follows:

airframe/ground –	FIX JOINT
AD pinion gear/airframe –	REVOLUTE JOINT
AD pinion gear/airframe –	MOTION
AD/link --	INLINE JPRIM (qty 2)
Link/FD --	REVOLUTE JOINT (fwd)
Link/FD --	CYLINDRICAL JOINT (aft)
AD/airframe --	VFORCE (rollers -- qty. 8)
AD/pinion gear --	GFORCE (gear drive -- qty. 10)
FD/FD --	BUSHING (hinges – qty 64)
FD/airframe --	VFORCE (rollers – qty 18)
AD.FD.pinion,airframe/ground	(gravity)



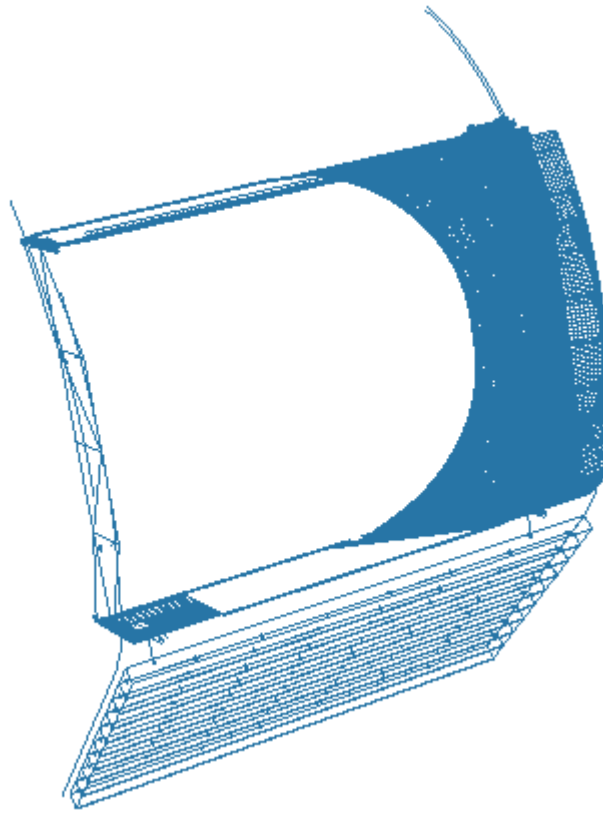


Fig. 6 AD-FD Assembly

### Constraints

The Airframe and AD attachment and gear drive schemes are similar to those for the URD. The forward connection between the AD and the first FD component is accomplished using a link PART pivoted to the FD with a REVOLUTE joint and to the AD using an INLINE JPRIM (ref, fig. 7). The inline JPRIM constrains the upper end of the link to move along the axis of the slide. The instantaneous contact position is determined by the position and force state of the system at any point in time. The aft link attachment is identical, except that the REVOLUTE is replaced by a CYLINDRICAL joint to prevent redundant constraints in the AD/FD attachment.

### Restraints

The roller/track interactions are similar to those for the URD, as are the gear drive forces. It should be noted that there are no thrust forces on the FD rollers, which assumes that sufficient tolerance exists so that the ends of the FD (radial) rollers cannot scrape the track faces.

The FD segments are connected together at each hinge location using ADAMS BUSHING elements (ref. fig. 8).

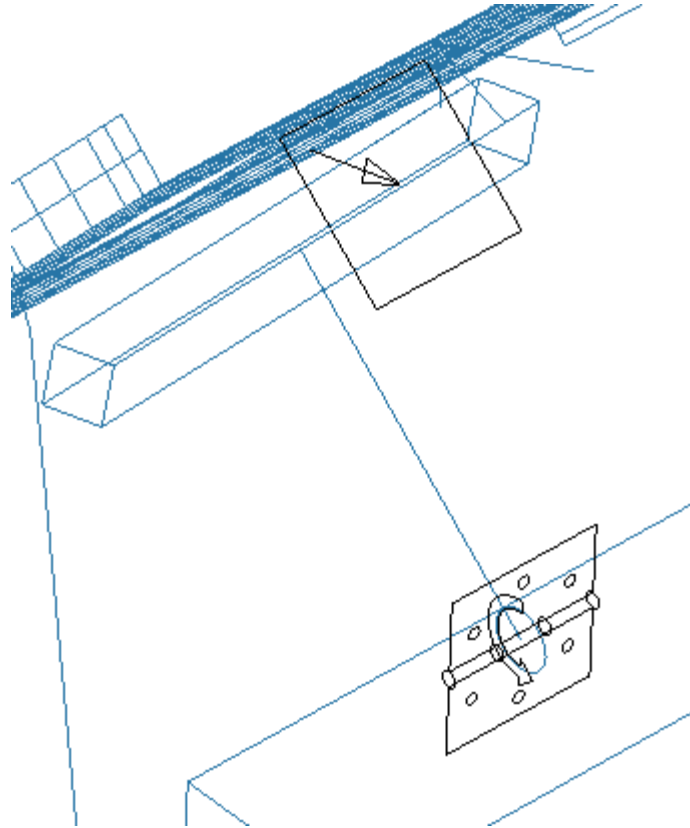


Fig. 7 AD/FD fwd Link Attachment

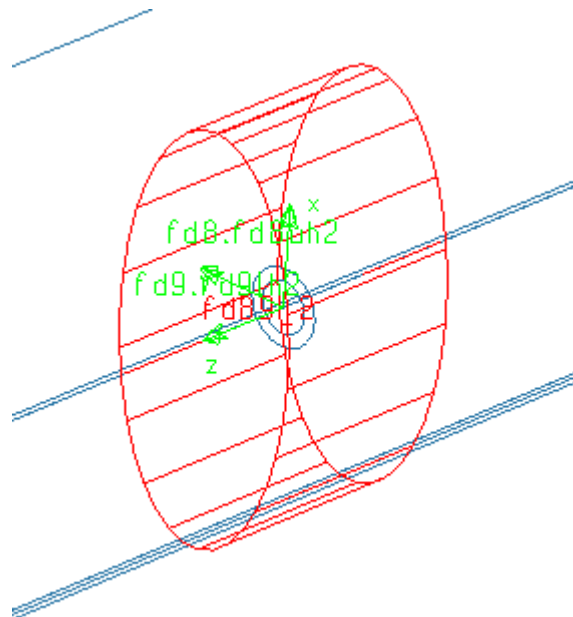


Fig. 8 Typical BUSHING Model of FD/FD Hinge

### Applied Loading

#### a) Aerodynamic Force

(Aerodynamic loads applied in Phase 1)

#### b) Gravity

The standard gravitational field of  $-386.088 \text{ in/sec}^2$  are applied to all PARTs.

### **Analysis Results-URD – Phase 1**

Figs. 9 and 10 show the URD in the fully-closed and fully opened positions. Shell images generated from

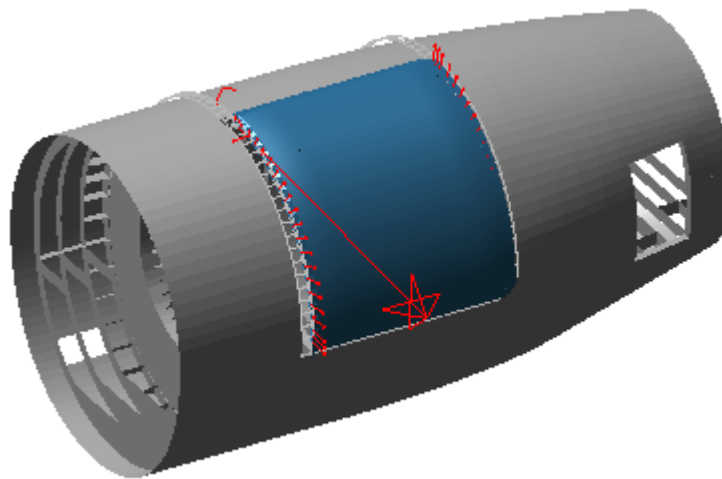


Fig. 9 URD Door in Fully Closed Position

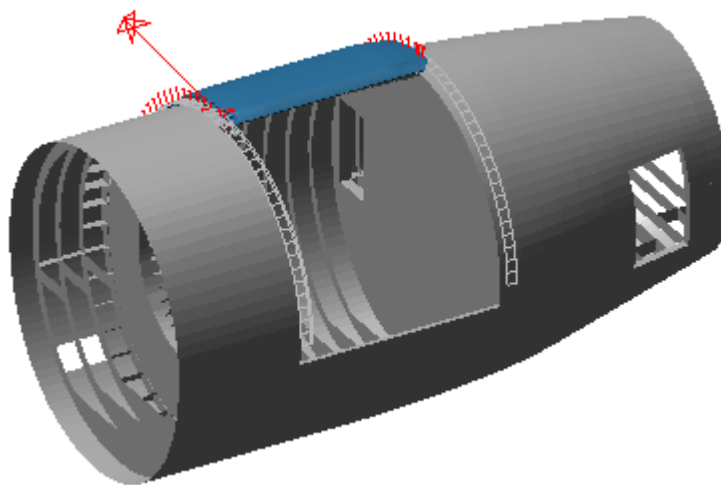


Fig. 10 URD in Fully Opened Position

FEA models of the aft airframe and URD were used to enhance the image. Figs. 11 and 12 give typical roller and gear drive loading for this, benign, load case.

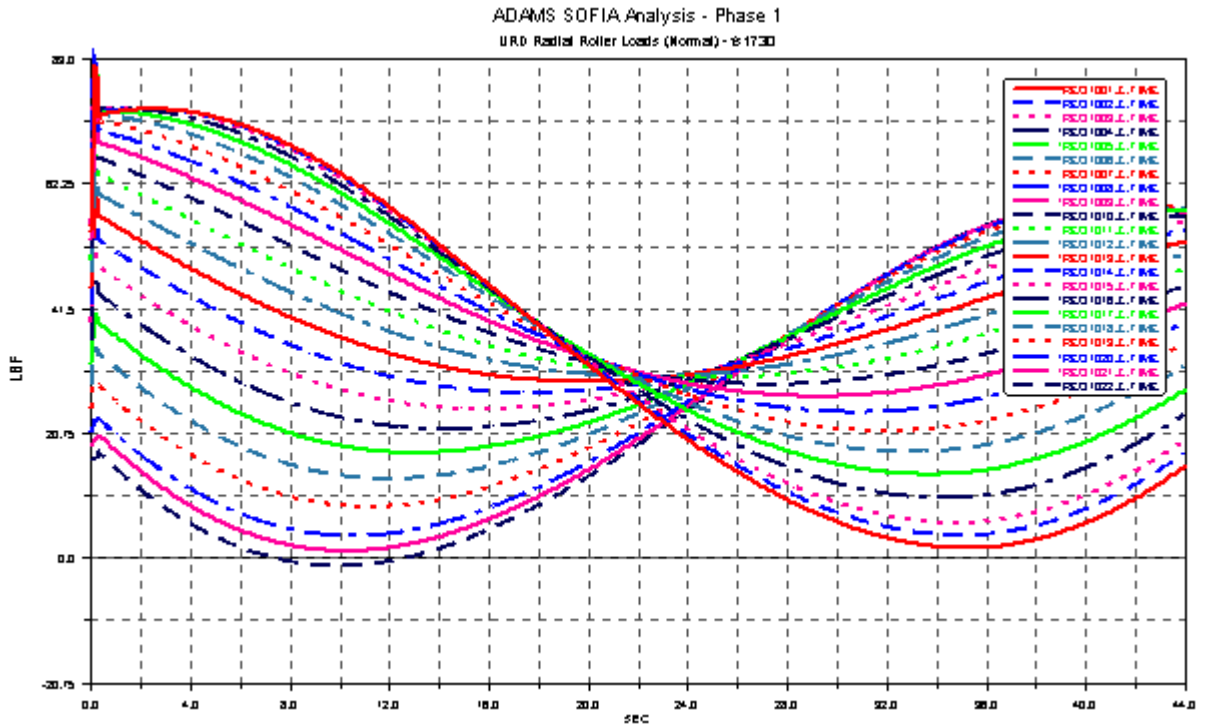


Fig. 11 URD Radial Roller Normal Loads – fs 1730

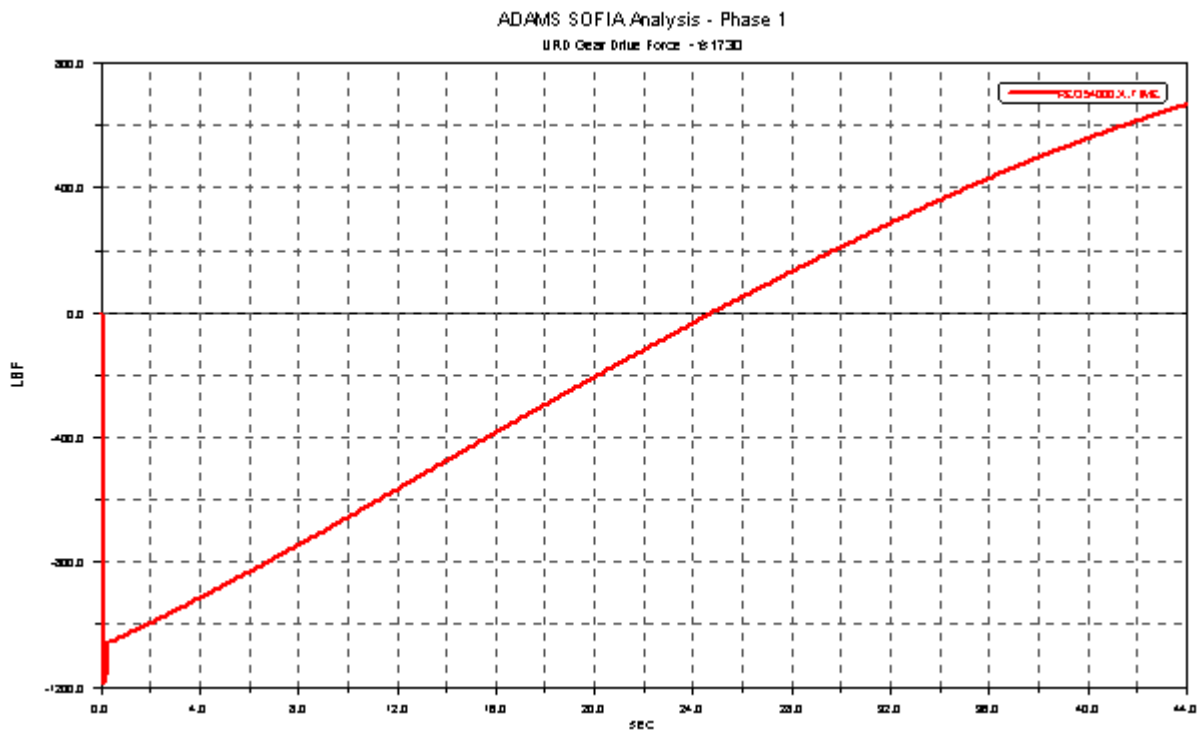


Fig. 12 URD Gear Drive Force – fs1730

## Analysis Results-AD/FD – Phase 1

Fig. 13 shows the AD/FD system fully open. As mentioned, the loading for phase 1 was benign and

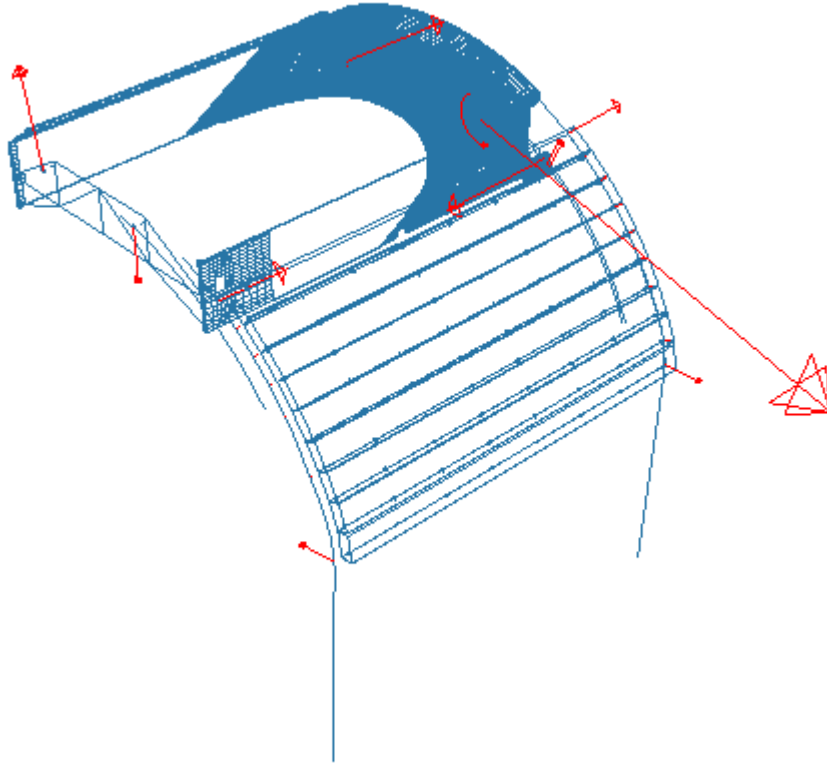


Fig. 13 AD/FD System Fully Opened

revealed modest loading in all rollers and in the gear drive systems. The AD/FD results exhibited a high-frequency oscillation of the links attaching the FD assembly to the AD. The links tended to 'hunt' rapidly up and down their slider attachments. This vibration propagated through the entire system. Closer examination revealed that the AD/FD attachment was incorrectly modeled. The pivoting attachment links (ref. fig. 7) were, in fact, bolted securely to the upper flexible door component. The error had introduced spurious degrees of freedom into the system. When the geometry was corrected, the oscillation disappeared.

## Phase II -- Flexible PEDS Components

### Upper Rigid Door (URD) NASTRAN Condensation

Fig. 14 below shows the 1<sup>st</sup> condensed mode of the URD. To keep the ADAMS model size small, only 6 hardpoints were employed (3 along the forward and aft edges) together with 6 fixed interface point eigenmodes, for a total of 42 elastic degrees-of-freedom..

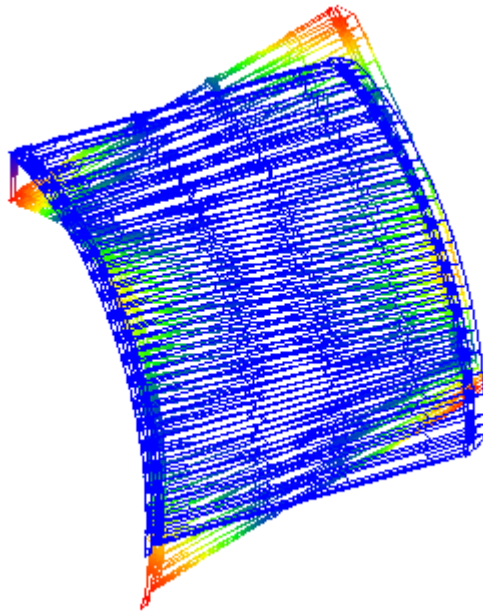


Fig. 14 Condensed URD 1<sup>st</sup> Structural (Free-Free) Mode 13.196 hz

### Aperture Door (AD) Modal Condensation

Fig. 15 gives the first free-free eigenmode for the AD model. These results show the

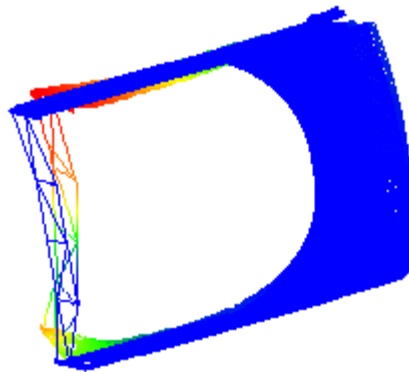


Fig. 15 AD 1<sup>st</sup> (Free-Free) Mode 3.073 hz

structure to be rather compliant. All attempts to employ the condensed structure inside an isolated ADAMS analysis were unsuccessful. Further scrutiny of the model lead to the discovery that the (supposed) rigid body modes associated with the Craig-Bampton points contained appreciable structural deformation. Fig 16 shows the 4<sup>th</sup> (supposed) rigid body mode at 0.000161 hz. The obvious structural deformation associated

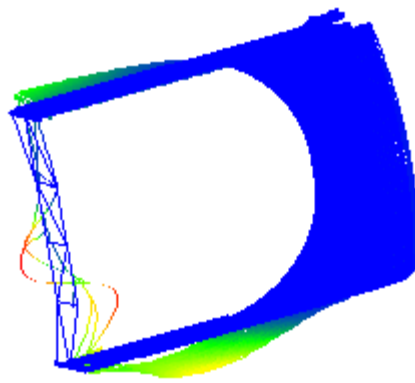


Fig.16 AD (Supposed) Rigid Body Mode at 0.000161 hz

with this rigid body mode cannot be correct and is a strong indicator that the NASTRAN model is not mathematically well conditioned for condensation and subsequent solution. Further basis for this claim can be found in the fact that all attempts to orthonormalize the condensed structure inside NASTRAN (the preferred method) met with failure. This forced a VIEW-based orthonormalization which, while successful in creating the condensed structure, obviously did not yield a well-conditioned one. As a result of this problem, the Phase 2 PEDS model of the Aperture Door system has been executed with the AD structure left rigid.

### Flexible Door (FD) Modal Condensation – General

Three different structures are combined to make the FD assembly. The top segment is typical of all of the segments but attaches to the bottom of the AD at two locations. The seven intermediate segments have eight hinge points top and bottom. The ninth segment has 8 hinges at the top and a thrust roller (which serves for the whole assembly) at its aft edge. Figure 17 shows the 1<sup>st</sup> structural mode for the top FD

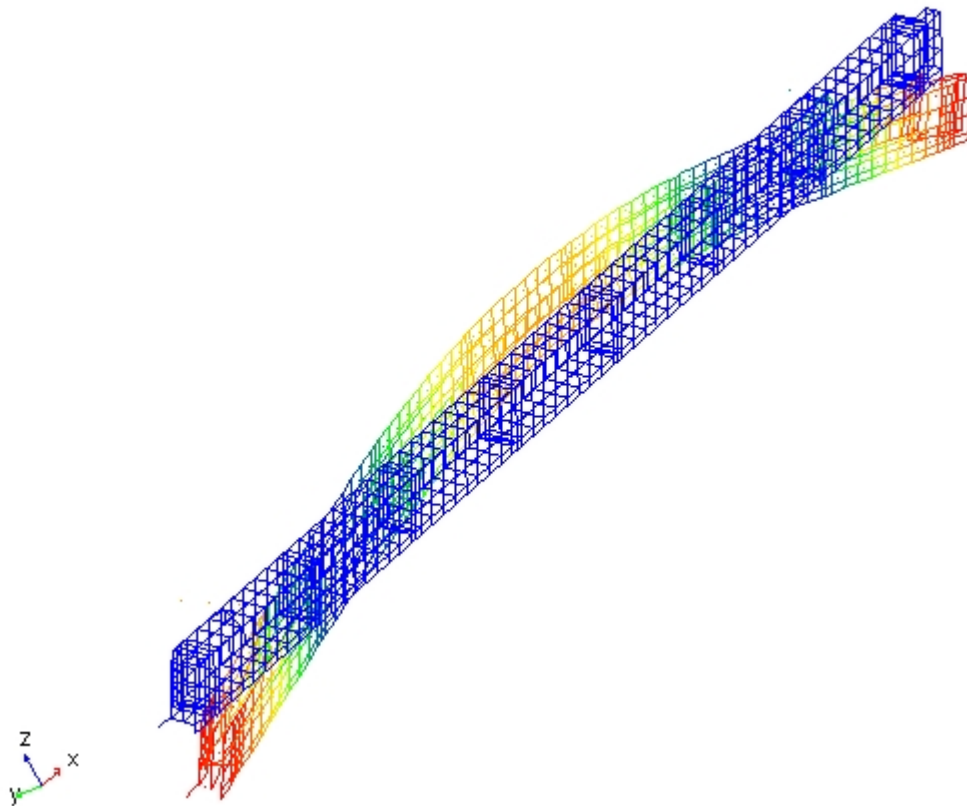


Fig. 17 FD 1<sup>st</sup> Segment 1<sup>st</sup> Free-Free Eigenmode 41.268 hz

segment This segment is somewhat heavier than the remaining 8 and is also stiffer, based on the frequency results.

## **FLEX\_BODY Incorporation**

Once the modal neutral file (.mnf) has been created and verified against the original structure, it must be incorporated into the system model. The process used in the PEDS modeling consists, in effect, of overlaying the flexible body on top of the rigid component it is to replace, transferring any system connections from the rigid part to the flexible part, and then deleting the rigid part. This was accomplished using an ADAMS/View command file (.cmd) to build the (rigid) phase 1 URD system model and then convert the URD structure to flexible. A typical creation sequence for the rigid (Phase 1) URD model is given below. Under the model name of "urd\_flex" a rigid PART named 'urd' is created, a (fwd) radial roller track reference MARKER is created (in aircraft coordinates), and the 14<sup>th</sup> radial urd roller is created relative to it in cylindrical coordinates.

```
part create rigid_body name_and_position &
  adams_id = 3 &
  part_name = .urd_flex.urd &
  ground_part = no

marker create &
  adams_id = 1 &
  marker_name = .urd_flex.airfrm.fs1730ref &
  location = 1753.29,0.0,231.0 &
  orientation = -90,90,0

marker create &
  marker_name = .urd_flex.airfrm.fs1730ads14 &
  location = 130.15,58.5,8.0
```

At this stage, the entries for a rigid model would be finished. To change the ADAMS PART just created to a FLEX\_BODY, the flexible part is created from the modal neutral file, markers are created on the FLEX\_BODY at the appropriate NASTRAN GRID locations, and a dummy (massless) PART and attachment marker are attached by a FIXED joint to the FLEX\_BODY at this location. This last step is done for purposes of modeling generality and computational efficiency. It should be noted that is common practice to 'tag' the dummy PART with the NASTRAN GRID ID for convenience. Finally, the roller marker originally created for the rigid part is transferred to the appropriate dummy part on the FLEX\_BODY and, after all system connections have been severed, the original, rigid part is discarded.

```
part create flexible_body name_and_position flexible_body_name=.urd_flex.urdf&
modal_neutral_file_name="urd.mnf" &
location=1838.5,0.0,0.0 orientation=0.0,0.0,0.0 relative_to=.urd_flex.ground &
invariants=yes,yes,yes,yes,yes,yes,yes,yes,no &
damping_ratio="user(.01,10,.1,20,1.0)"

marker create marker_name=.urd_flex.urdf.g306131 node_id=306131

part create rigid_body name_and_position part_name=.urd_flex.g306131&
orientation=0.0,0.0,0.0 relative_to=.urd_flex
marker create marker_name=.urd_flex.g306131.g306131 &
orientation=0.0,0.0,0.0 relative_to=.urd_flex.urdf.g306131
constraint create joint fixed joint_name=.urd_flex.a306131j &
i_marker_name=.urd_flex.g306131.g306131&
j_marker_name=.urd_flex.urdf.g306131

marker modify marker_name=.urd_flex.urd.fs1730urd14r &
  new_marker_name=.urd_flex.g306131.fs1730urd14r

part delete part_name=urd
```



## Aerodynamic Loads

At the time this work was completed, the ADAMS MFORCE was not available to apply distributed loading, and the aerodynamic loads on the various surfaces had to be lumped to keep the model size reasonable. For the URD, a 4 X 4 grid was employed (ref. fig 18). The loads at these lumped locations are applied using ACTIONONLY SFORCEs. These are single component forces oriented along the Z-axis of the

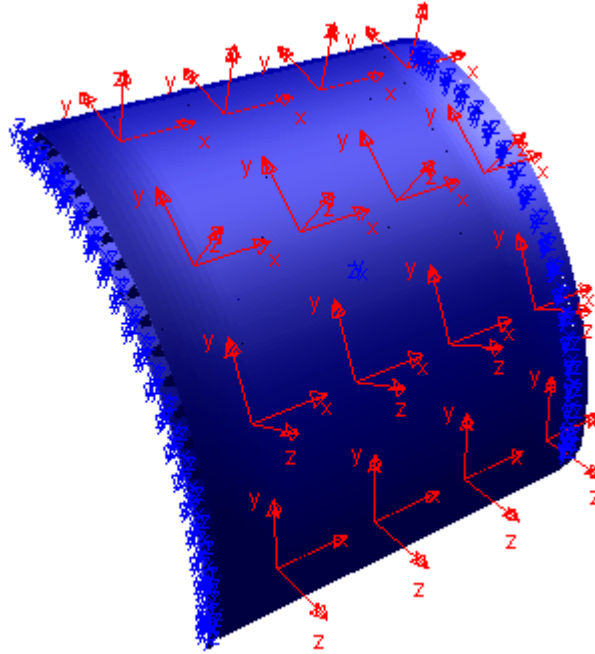


Fig. 18 URD Aerodynamic Loading Grid

reference triad used to locate them. These forces are applied as 'actions', which means they must be reacted by other forces (e.g., the retention forces of the rollers) in the system. The force values supplied to the SFORCEs are input using ADAMS SPLINE functions which interpolate the aero force as a function of the (angular) door position. A typical ADAMS dataset aero SFORCE (one of 16 total) and its related SPLINE function are:

```
!                                adams_view_name='urdall_aero'
SFORCE/15011, TRANSLATIONAL, I = 15011, J = 15011, ACTIONONLY
, FUNCTION = akispl(ax(15001,15000)*rtod,0,15011)
!

!                                adams_view_name='SPL15011'
!                                adams_view_units='no_units'
SPLINE/15011, X = 0, 5.32, 29.92, 52.56, 76.18, 102.47, 110, Y = 4375, 4375
, 4375, 4375, 4375, 4375, 4375
!
```

The force expression requires that the angular rotation about the (airframe) X-axis of (door fixed) MARKER 15001 relative to (airframe fixed) MARKER 15000 be converted from radians to degrees and that this value be used as the abscissa (X-) value in SPLINE 15001. Although the lumped aero forces were configured to be variable with position, constant loads, summing to 70000lbf (radial) were used.

It should be emphasized that the points of aero load application are not Craig-Bampton points. This fact enables a smaller, faster-computing model and is justified on the grounds that the aero loads are, in reality, distributed and can be adequately represented by the distributed, modal flexibility of the structure. The aero loads on the AD and the FD segments were applied in a similar fashion.

During a review of the system it was discovered that a thrust roller on the 9<sup>th</sup> FD segment had never been incorporated into the model. This was added, and all of the track and gear drive geometry was reviewed and corrected, if necessary.

## Analysis Results URD -- Phase 2

Figs. 19 shows the URD in the fully closed position while figs. 20 and 21 give two views of it fully opened.

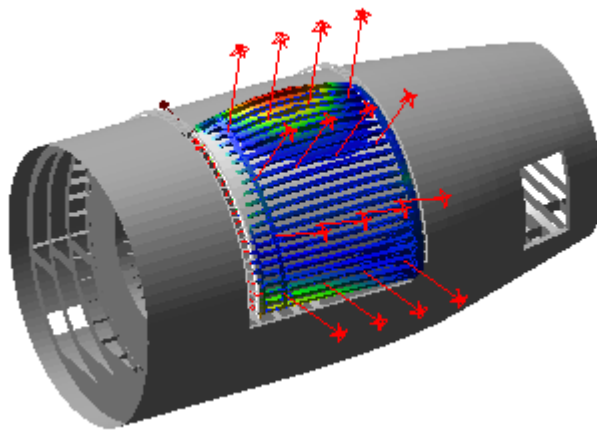


Fig. 19 URD (Phase 2) in Fully Closed Position

The contour plots are of deformations, not stresses. The deflections of the flexible URD have been amplified by a factor of 20 to more clearly show the deformation shape of the door structure.

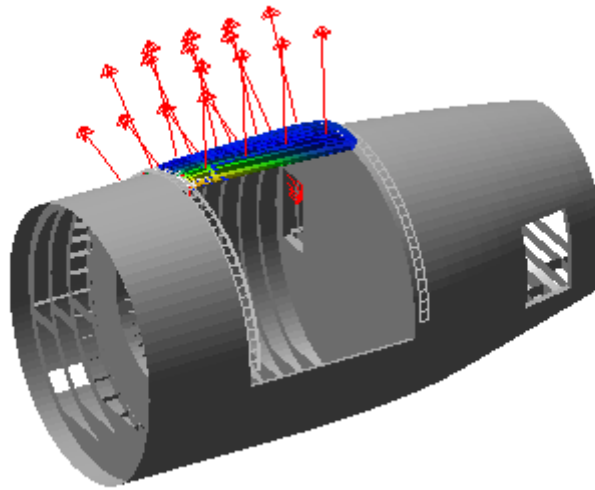


Fig. 20 URD (Phase 2) in Fully Opened Position (From Port Side)

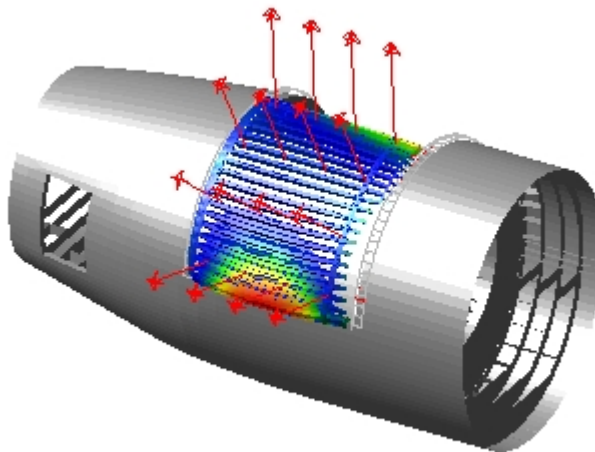


Fig. 21 URD (Phase 2) in Fully Opened Position (From Starboard Side)

The roller, track, and gear drive loads, while substantially higher than for the benign loading of phase 1, still appeared within structural limits. For the sake of functional redundancy, it was recommended that an additional thrust roller be added to each thrust roller position on the forward edge of the door.

## Analysis Results AD/FD – Phase 2

Figs. 22 and 23 show the AD/FD in the full down and fully elevated positions, respectively. The fuselage for this phase is still rigid, and a shell file has been employed to represent it graphically.

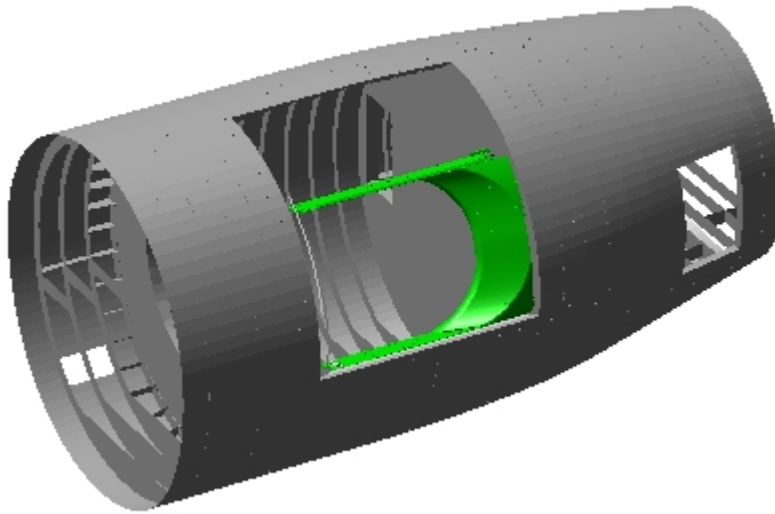


Fig. 22 AD/FD (Phase 2) in Fully Closed Position

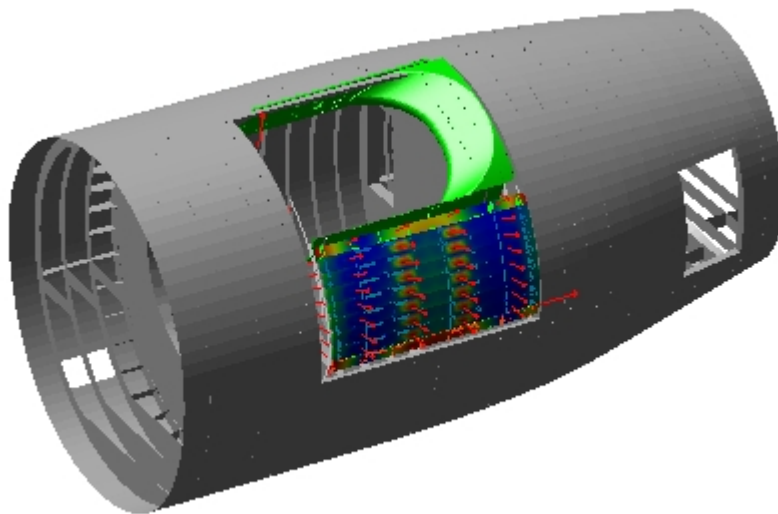
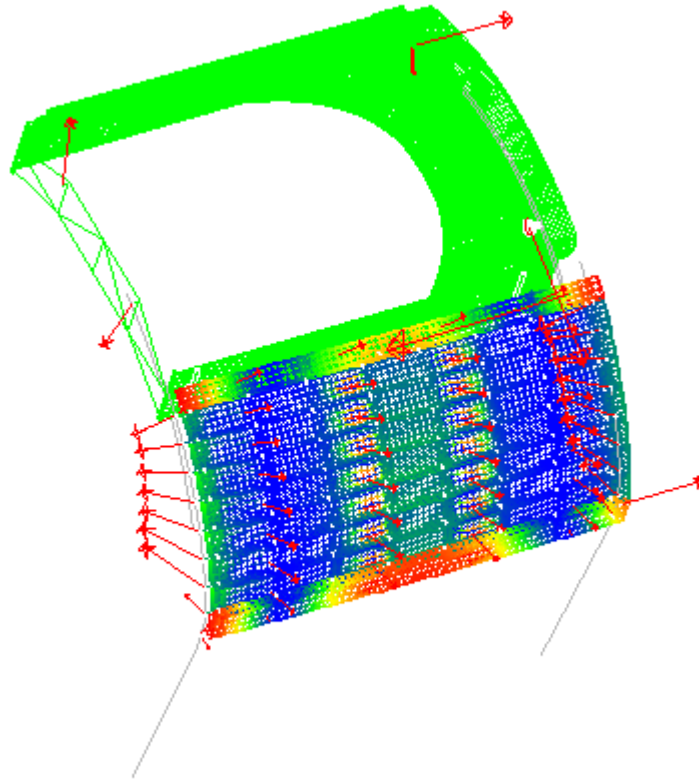


Fig. 23 AD/FD (Phase 2) in Fully Opened Position

Aerodynamic loads for the AD were not available and, thus, were not applied. Estimated aerodynamic loads (based on a +2 psi overpressure) have been applied to each FD segment. They have a value of zero while still in the cavity below the lower cavity sill, but are stepped up to full value over a distance of a few

inches upon clearing the cavity. Fig. 24 shows AD/FD system in the elevated position with the airframe



removed for clarity.

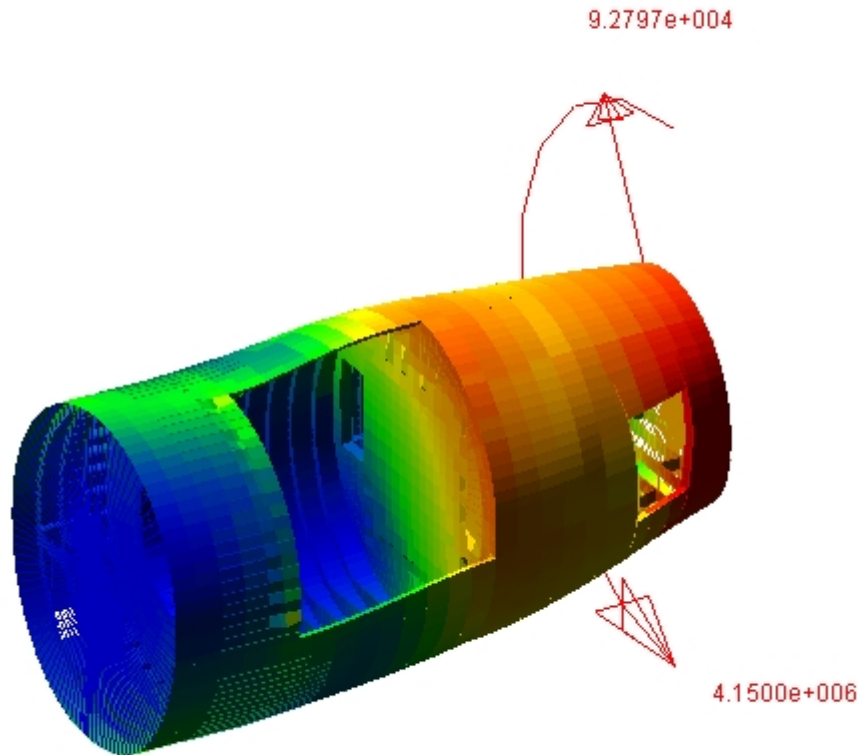
Fig 24 AD/FD System in Elevated Position (Airframe Graphics Removed)

Even with the AD aerodynamic loads absent, because of the addition of the aerodynamic loading on the FD components, the attachment loads between the AD and the first FD segment rose appreciably. A recommendation was made to scrutinize the AD structure in a Finite Element Analysis employing the ADAMS-derived loading.

### Phase 3 Modeling (Suspended)

#### Airframe Deformation Study

Before commencing with the actual incorporation of the flexible airframe into the complete system, an exploratory model of the airframe section alone was created to examine its behavior when subjected to (simulated) empennage loads. Fig 25 shows the airframe under an assumed loading. The deformation contours have been amplified by a factor of 50. The aperture deformations resulting from the loading



Fig, 25 Provisional Airframe Distortion under Assumed Empennage Loading

appear reasonable. Preliminary work had begun on modeling the flexible URD to the flexible aft fuselage when work on Phase 3 was suspended by RSC because of proposed design changes to the system.

### Phase 3 (Modified) Flexible URD – Pseudo Flexible Aft Fuselage

Because of configuration issues associated with the PEDS and the unavailability of an aft fuselage NASTRAN finite-element model inclusive of all the moving component track structure, RSC made the decision to complete a rapid analysis using a "pseudo flexible" airframe to estimate the effect of airframe deformation on the roller loading of the URD (only) system. To accomplish this, the aft airframe was broken into two, discrete, rigid bodies which were then connected together by a 6 degree-of-freedom, controllable coupler initially located at the midpoint of the telescope aperture (fuselage station 1825, water line 231, butt line 0). Fig. 26 shows the initial model of this system,

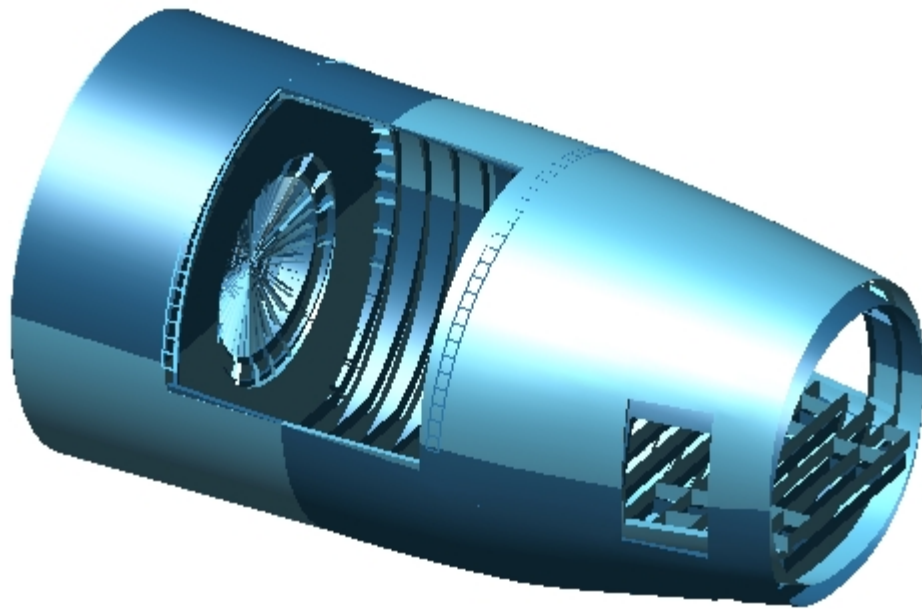


Fig. 26 Deflected Pseudo-Flexible Airframe

minus the URD door. Duplicate shell graphics of the entire fuselage section have been employed for both airframe parts and the aft portion of the airframe (dark blue) has been deflected by the coupler (an exaggerated) 3 degrees tail down in pitch (only) with respect to the front part of the airframe (light blue). An estimate of the amount of structural deflection this represents can be obtained from the skin shading and from the overlap in the aft door cutout and from comparing the relative positions of the aft fuselage frames. When this preliminary analysis proved the approach to be viable, a more detailed analysis was performed to more rationally locate the component coupler and to set the coupler deflections to match, as closely as possible, the aft fuselage deflections predicted by a NASTRAN model of the entire airframe.

### **Aperture Deformation – Elastic Airframe**

Figure 27 shows the aft fuselage structure with the corner grids of the aperture displayed. RSC selected critical load case condition #3 from the "Critical Conditions" loading chart (DM6001 BA006-00-25 Balanced Maneuver at VD 2.5g up). The deflections of the aperture corners under this loading are given in table 1.

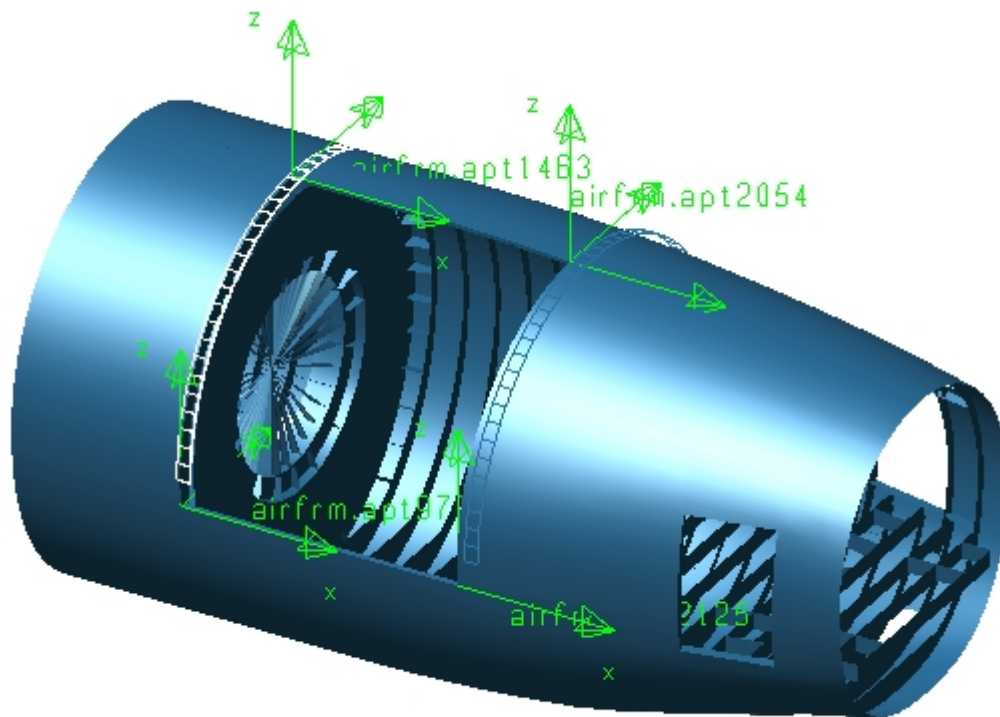


Fig. 27 Aperture Corner Grids

Aperture Corner Deformations (in Inches) Due to Load Condition #3 DM_6001 Balanced Maneuver				
GRID	972	1463	2054	2125
X	+0.085	+0.807	+1.116	+0.274
Y	+0.140	-0.005	-0.351	-0.232
Z	-1.541	-1.705	-3.965	-3.988

Table 1 Aperture Corner Deformations – Condition #3 – 2.5g

Because the airframe model here is only partial and is not truly elastic, these deformations must be re-referenced to obtain, in effect, the aft corner displacements with respect to the forward corner displacements. To accomplish this, the corner deformations were 'normalized' with respect to GRID 972 by subtracting its (translational) deformations from those of the other locations. Table 2 gives the normalized deformations.

Aperture Corner Deformations (in Inches) Due to Load Condition #3 -- Normalized to GRID 972				
GRID	972	1463	2054	2125
X	0.0	+0.722	+1.031	+0.089
Y	0.0	-0.145	-0.491	-0.372
Z	0.0	-0.164	-2.242	-2.447

Table 2 Normalized Aperture Corner Deformations – Condition #3 – 2.5g



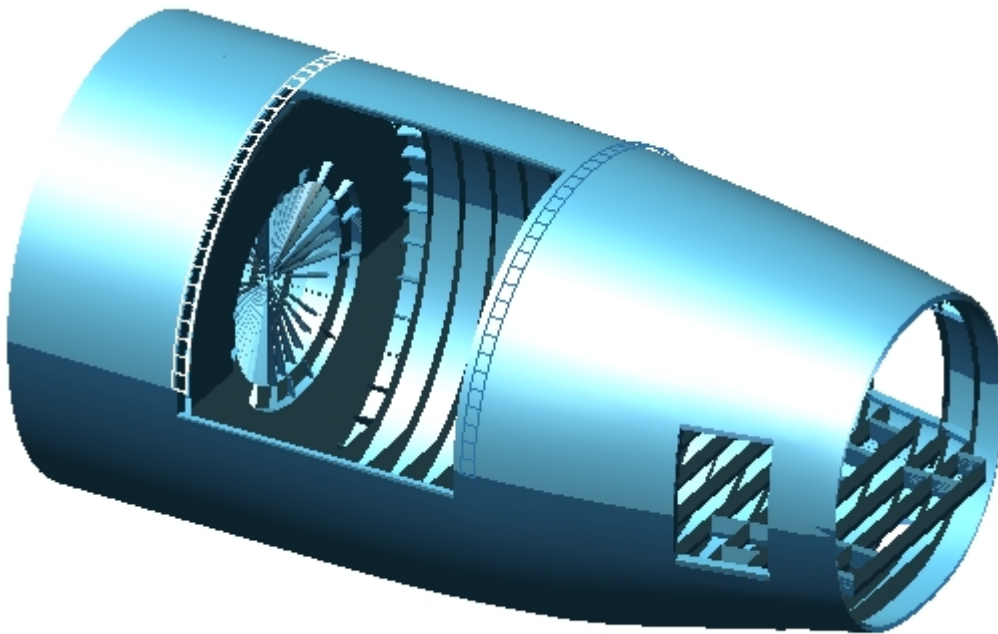


Fig. 28 Deformed Pseudo-elastic Structure Under Load Condition #3

Based on this analysis, the 'pseudo-elastic' representation of the airframe deflection is accomplished by moving the positionable coupler to fuselage station fs1746, water line wl 212.714, butt line bl 0.0 and applying to it a bending displacement of 0.382deg. and a shearing deformation of 1.281 inches. Figure 28 shows the aft airframe under these conditions and table 3 gives the corner deformations computed from them. Note that these deformations should be matched against the normalized values in table 2.

<b>Pseudo-elastic Aperture Corner Deformations (in Inches) Due to Load Condition #3</b>				
<b>GRID</b>	<b>972</b>	<b>1463</b>	<b>2054</b>	<b>2125</b>
<b>X</b>	0.0	0.0	+0.946	-0.003
<b>Y</b>	0.0	0.0	0.0	0.0
<b>Z</b>	0.0	0.0	-2.441	-2.441

Table 3 Pseudo-elastic Aperture Corner Deformations – Condition #3 – 2.5g

Fig. 29 gives an angled, close-up of the lower edge of the aperture. The light blue band running along the bottom edge of the aperture gives an indication of the aperture deformation. The effective deformation is that associated with a line running from the top of the blue band at the forward position to the bottom of the blue band at the aft end.

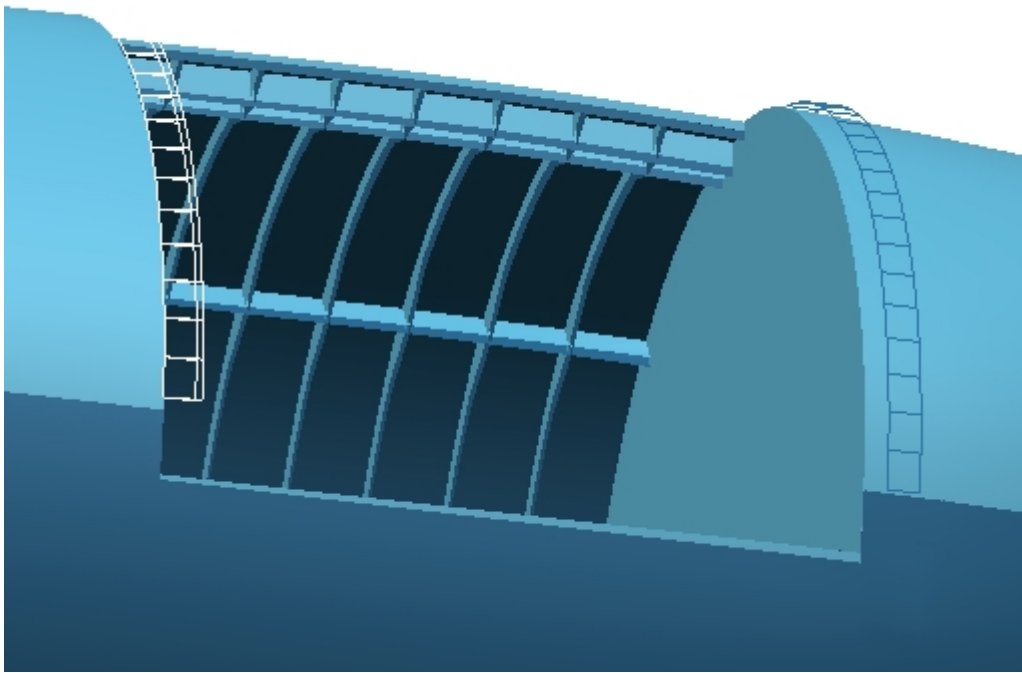


Fig. 29. Close-up of Lower Aperture Edge

In addition to the airframe deformations given above, the applied loading included a 2.5g gravitational loading ( $-965.22 \text{ in/sec}^2$  down) and, lumped, normal pressure loading on the URD of 4375 lbf at 16 locations. 32 Elastic modes (from 13.92 hz up to 4205 hz) were employed to represent the URD elasticity. Fig. 30 shows the URD displayed in 80-degree open position.

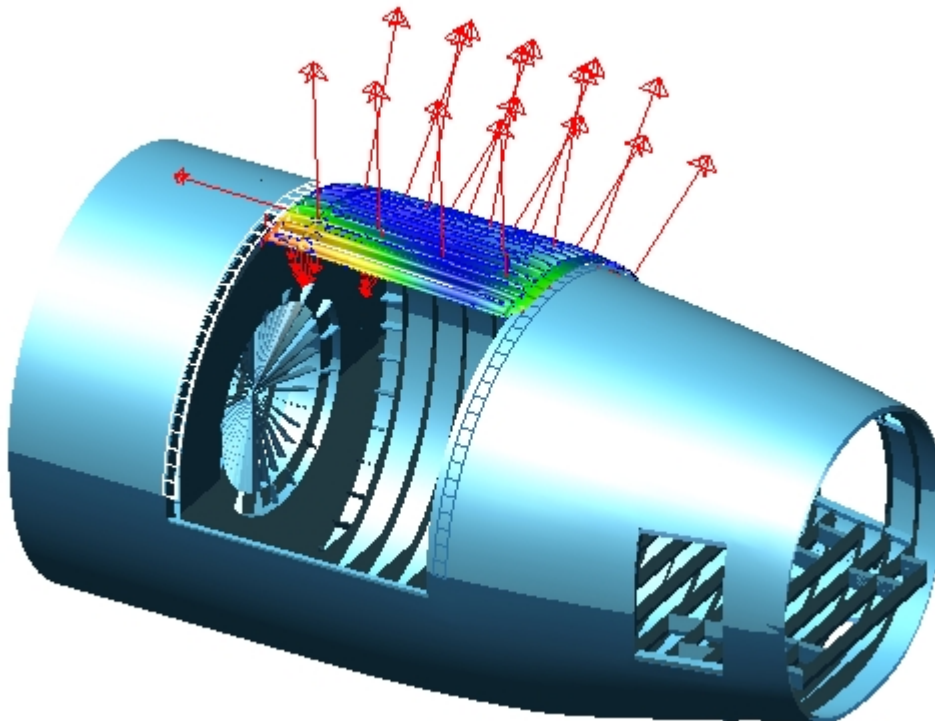


Fig. 30 URD At 80-Degree Position -- Condition #3 -- 2.5g

## Analysis Results – Phase 3m

The inclusion of the (pseudo) airframe deformations for the 2.5-G case had a dramatic effect on the URD system loads. The thrust rollers exhibited roller loads well beyond the maximum permissible allowable. This served to reinforce the earlier recommendation that additional thrust rollers be added to the forward URD edge.

## Conclusions

The ADAMS analysis performed on the SOFIA PEDS configuration gives a detailed picture of the operational forces arising internally in the system as well as the loading experienced by the airframe which mounts it. The addition of airframe flexural effects (estimated) leads to a dramatic increase in loading experienced by the URD. As soon as the proposed design changes to the PEDS are completed, the analysis should be repeated for all components (URD/AD/FD) to confirm their integrity. The analysis should be expanded to employ the fully elastic airframe, as originally intended.

## BIBLIOGRAPHY

- 1) Using ADAMS/Solver Version 9, (anon.), Mechanical Dynamics, Inc. Ann Arbor, MI 1997
- 2) Using ADAMS/View Version 9, (anon.), Mechanical Dynamics, Inc. Ann Arbor, MI 1997
- 3) MSC/NASTRAN Quick Reference Guide Version 69, Reymond, M., M. Miller Ed., MacNeal-Schwendler Corp., Los Angeles, CA, 1996